ISSN: 1410-8917
e-ISSN: 2597-9914

Jurnal Kimia Sains dan Aplikasi 27 (1) (2024): 28-34

Jurnal Kimia Sains dan Aplikasi
Journal of Scientific and Applied Chemistry

Journal homepage: http://ejournal.undip.ac.id/index.php/ksa

Synthesis of Molecularly Imprinted Polymers with Magnetite Cores for Ibuprofen Adsorption

Halimah Fahri [1,*], Muhammad Ali Zulfikar [1], Muhammad Yudhistira Azis [1]

[1] Department of Chemistry, Faculty of Sciences and Mathematics, Bandung Institute of Technology, Bandung, Indonesia

* Corresponding author: halimahlily5@gmail.com

https://doi.org/10.14710/jksa.27.1.28-34

Article Info

Article history:

Received: 13th July 2023
Revised: 04th February 2024
Accepted: 13th February 2024
Online: 19th February 2024

Keywords:
ibuprofen; magnetic; adsorption; molecularly imprinted polymers

Abstract

Ibuprofen (IBP) is a pollutant that is widely found in aquatic environments due to pharmaceutical waste and the metabolic results of humans who consume the drug. These compounds can cause damage to aquatic ecosystems, genotoxicity, and aquatic toxicity and are harmful to human health. This study aims to selectively adsorb IBP using magnetic molecularly imprinted polymers (MMIPs) synthesized from ibuprofen (IBP) as a template molecule, methacrylic acid (MAA) as a functional monomer, and divinylbenzene (DVB) as a crosslinker with a mole ratio of 1:4:20 in acetonitrile porogen solvent using a bulk polymerization method. Fe_3O_4 nanoparticles and MMIPs were characterized using X-ray Diffraction (XRD), Fourier Transform Infra-Red (FTIR), and Scanning Electron Microscope (SEM). IBP adsorption reached optimum conditions at pH 3 with a contact time of 90 minutes and a mass of 25 mg of adsorbent. The adsorption performance of MMIPs for IBP was evaluated by adsorption isotherms and adsorption kinetics. Adsorption of IBP by MMIPs followed the Langmuir adsorption isotherm model with an adsorption capacity of 227.24 mg/g. Kinetic studies showed that the adsorption process followed a pseudo-second-order adsorption kinetic model. MMIPs can adsorb IBP selectively even in the presence of interfering compounds, are easily separated from the solution, and can be used repeatedly with good adsorption ability. Hence, it is efficient and promising for removing IBP from aqueous media.

1. Introduction

Ibuprofen (IBP) is a pharmaceutical preparation of an acidic nature that belongs to the class of nonsteroidal anti-inflammatory drugs (NSAIDs), widely used to address inflammation and as an analgesic, antipyretic, and antirheumatic agent [1, 2]. The high consumption rate of this compound has led to the widespread detection of ibuprofen in the environment, originating from various sources such as domestic and industrial wastewater, sludge from wastewater treatment plants, hospitals and pharmaceutical manufacturing facilities, aquaculture, farming, and landfill sites [3]. Additionally, wastewater treatment plants (WWTPs) have found elevated concentrations of these drugs, originating from human metabolic excretions resulting from the consumption of these medications [4]. The presence of this compound in water can pose serious problems for the environment and human health, as it can cause genotoxicity, water toxicity, and resistance to pathogenic bacteria [5].

Several methods have been employed to remove IBP, including filtration, electrocoagulation, ozonation, photocatalysis, and adsorption [6, 7]. However, in their application, these methods are only efficient for some medications, the reaction time is not sufficiently short, intermediate/oxidized products are not adequately degraded, and the resulting oxidation by-products have high toxicity levels that can worsen environmental and human health impacts [3]. Adsorption is the most popular method for removing organic contaminants such as pharmaceuticals because it is highly effective, simple, relatively inexpensive, and does not cause secondary water pollution [8]. Some adsorbents used for IBP adsorption include porous adsorbents such as clays and minerals, activated clay, activated carbon, graphene

oxides, and others [9]. However, all these adsorbents have relatively low selectivity [10].

Molecularly imprinted polymers (MIPs) are adsorbents known for their high selectivity and ability to identify target compounds selectively [11]. MIPs are synthesized through the polymerization of functional monomers and crosslinkers in the presence of the template molecule. The polymer creates cavities upon the release of the template molecule, which is used to bind the target molecules [12]. The advantages of MIPs include high selectivity, stability, easy preparation, low cost, and reusability [12, 13]. However, MIPs are challenging to separate from their solution, requiring significant time. Therefore, MIPs are modified with magnetic particles (MMIPs) to facilitate separation using an external magnet without requiring centrifugation or filtration, allowing quick binding and separation [14]. Additionally, by incorporating magnetite particles, the resulting polymer can be nano-sized, as magnetite serves as the core, leading to uniform shapes without grinding [15, 16].

In this study, the adsorption of IBP was conducted using molecularly imprinted magnetic polymers (MMIPs) synthesized from ibuprofen (IBP) as a template molecule, methacrylic acid (MAA) as a functional monomer, divinylbenzene (DVB) as a crosslinker, benzoyl peroxide (BPO) as an initiator, and acetonitrile as a porogen. Subsequently, the synthesized MMIPs were characterized using XRD, FTIR, and SEM. The adsorption performance of MMIPs was also evaluated using adsorption isotherm models, adsorption kinetics, selectivity studies, and regeneration studies.

2. Experimental

This research was conducted through several experimental stages, starting with the synthesis of Fe_3O_4 nanoparticles, followed by the synthesis of magnetic molecularly imprinted polymers (MMIPs) and their characterization. Subsequently, MMIPs were utilized in experiments for the adsorption of IBP, selectivity studies, and regeneration.

2.1. Materials

The materials used were ibuprofen (Aldrich, ≥98%), naproxen (Aldrich), methacrylic acid (Aldrich, 99%), divinylbenzene (Aldrich, 80%), polyvinylpyrrolidone (Aldrich, Mw 55,000), benzoyl peroxide (Merck 75%), $FeSO_4.7H_2O$ (Aldrich), $FeCl_3.6H_2O$ (Aldrich), NH_4OH, oleic acid, acetonitrile (Merck, ≥99.9%), HPLC-grade methanol (Merck, ≥99.9%), and deionized water.

2.2. Synthesis of Fe_3O_4 Nanoparticles

Nanoparticles Fe_3O_4 were synthesized by the coprecipitation method [16]. A 0.5580 g of $FeSO_4.7H_2O$ and 1.1160 g of $FeCl_3.6H_2O$ were dissolved in 100 mL of deionized water and stirred until homogenous at 80°C. Then, NH_4OH was added dropwise to the mixture with rapid stirring until a black precipitate formed (pH 9). The solution was stirred for 15 minutes, then 2 mL of oleic acid was added, followed by stirring for 15 minutes. The obtained precipitate of Fe_3O_4 nanoparticles was separated, washed several times with deionized water and ethanol, and then isolated from the solution using an external magnetic field. Subsequently, the Fe_3O_4 nanoparticles were dried in an oven at 60°C.

2.3. Synthesis of Magnetic Molecularly Imprinted Polymers (MMIPs)

The MMIPs were prepared using the bulk polymerization method [15, 16]. One mmol of IBP and 4 mmol of MAA were dissolved in 10 mL of acetonitrile and stirred to create a pre-polymerization solution. Next, 20 mmol of DVB and 1 g of Fe_3O_4 were added to the solution. Then, the PVP solution was added to the pre- polymerization solution. Following that, 150 mg of BPO was added to the solution while flowing nitrogen gas for 5 minutes to eliminate dissolved oxygen in the solution. Polymerization was carried out in an oil bath at 70°C with continuous stirring for 3 hours. The resulting MMIPs precipitate was separated from the solution using an external magnetic field and washed several times with acetonitrile. The template molecules within the polymer were extracted multiple times with an acetonitrile solution. After removing the template molecules, the MMIPs product was separated and dried in an oven at 60°C.

2.4. Material Characterizations

The size and crystallinity of Fe_3O_4 nanoparticles and MMIPs were determined using X-ray diffraction (XRD MiniFlex 300/600). The functional groups were identified using FT-IR Prestige-21 (Shimadzu, Japan) with a KBr pellet-type sample over the wavenumber range 4000-450 cm^{-1}. A scanning electron microscope (JEOL JSM-6510 LA) was used to observe the surface morphology of materials. Adsorption analysis was done using a UV-Vis Spectrophotometer at a wavelength of 222 nm.

2.5. Batch Adsorption Experiments

To investigate the adsorption capacity of the polymer, the influence of experimental parameters, namely pH (2–8), contact time (10–150 minutes), and adsorbent dose (10–30 mg) on the removal of IBP, were studied in batch mode. A stock solution was prepared by dissolving an accurate amount of IBP (99%) in a mixture of methanol and deionized water (1:1, v/v), and a working solution was prepared by dilution. In the adsorption isotherm study, 25 mg of MMIPs were added to 25 mL of IBP solution with varying initial concentrations from 40 to 300 mg/L. The solutions were left for 90 minutes at 298 K to reach adsorption equilibrium. After 90 minutes, MMIPs were separated from the solution using an external magnetic field. In the adsorption kinetics study, 25 mL of a solution with an initial IBP concentration of 50 mg/L was reacted with 25 mg of the adsorbent in batch experiments for various contact times (10–150 minutes), and the remaining IBP concentration in the solution was measured using a UV-Vis spectrophotometer at 222 nm. The percentage removal and adsorption capacity of IBP adsorbed into MMIPs were calculated using Equations (1) and (2).

$$q_e = \frac{(C_i - C_e)V}{m} \quad (1)$$

$$\%\ Removal = \frac{(C_i - C_e)}{C_i} \times 100\% \quad (2)$$

where q_e is the adsorption capacity (mg/g), C_i is the initial concentration of IBP (mg/L), C_e is the equilibrium concentration of IBP (mg/L), V is the volume of solution (L), and m is the sorbent mass (g) [17].

2.6. Selectivity Studies

The selectivity of MMIPs for IBP was tested with a solution containing the interfering compound NPX using two different methods. Firstly, in the adsorption of a single solution, 25 mg of MMIPs adsorbent was added to separate Erlenmeyer flasks, each containing 25 mL of IBP and NPX solutions with a concentration of 50 mg/L at pH 3. After adsorption for 90 minutes, IBP and NPX were detected using HPLC with UV detectors at 222 nm and 232 nm, respectively. Subsequently, in the adsorption of a binary solution, 25 mg of MMIPs were added to Erlenmeyer flasks, each containing 25 mL of a binary mixture of IBP and NPX solutions with concentration ratios (50:50, 50:100, and 100:50 mg/L) at pH 3, and reacted for 90 minutes. The supernatant was separated from the sorbent using an external magnetic field and analyzed with HPLC with a UV detector at 222 nm. Samples were separated by a C_8 column with a mobile phase of 50% methanol and 50% deionized water at a flow rate of 1 mL/minute.

2.7. Regeneration Studies

To study the regeneration performance of MMIPs for IBP adsorption, 25 mg of MMIPs were added to a 25 mL solution of 50 mg/L IBP, and the solution was left at 298 K for 90 minutes. After adsorption, MMIPs were separated using an external magnetic field, and the remaining amount of IBP in the solution was measured with a UV- Vis spectrophotometer at 222 nm. The MMIPs adsorbent was washed with 25 mL of eluent (methanol: acetonitrile = 1:1, v/v) for 12 hours.

3. Results and Discussion

Fe_3O_4 nanoparticles and MMIPs were characterized using XRD, FTIR, and SEM. Additionally, the adsorption performance of MMIPs towards IBP was evaluated using UV-Vis spectrophotometry and HPLC UV. Adsorption isotherms were determined using the Langmuir and Freundlich isotherm models, and adsorption kinetics were determined using pseudo-first-order and pseudo-second-order kinetics.

3.1. X-ray Diffraction (XRD) Characterization

The XRD patterns of Fe_3O_4 nanoparticles and MMIPs are presented in Figure 1. Dominant diffraction peaks appear at 2θ angles of 30.4°, 35.6°, 43.3°, 57.2°, and 63°, corresponding to the Miller index (220), (311), (400), (511), and (440), respectively. These peaks align with the reference pattern for Fe_3O_4 (COD 1010369), indicating that the synthesized structure of Fe_3O_4 nanoparticles is a cubic spinel. Similar XRD patterns were obtained for MMIPs [14], demonstrating the successful modification of MIPs with Fe_3O_4 nanoparticles. Furthermore, using the Debye-Scherrer equation [18], the average crystal size of Fe_3O_4 is estimated to be approximately 12.81 nm.

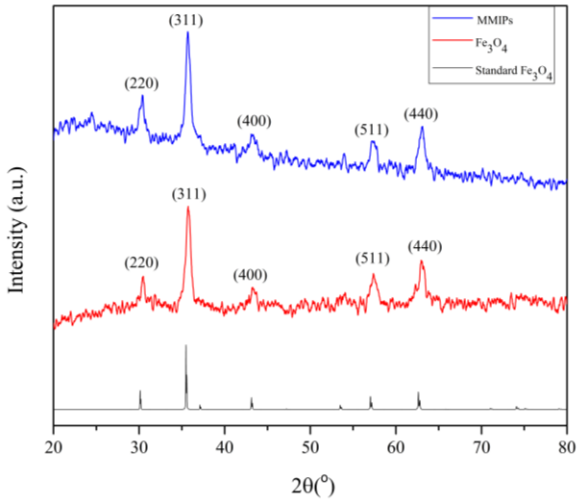

Figure 1. Diffractogram of Fe_3O_4 nanoparticles and MMIPs

3.2. Fourier Transform Infrared (FTIR) Characterization

Fe_3O_4 nanoparticles, MNIPs, and MMIPs were characterized using FTIR to identify functional groups, and the FTIR spectra are shown in Figure 2. Based on the spectra obtained in Figure 2, there is an absorption band at 589 cm^{-1} in all three spectra, which is characteristic of the Fe-O stretching vibration in Fe_3O_4 nanoparticles. The broad bands at 3380 and 3441 cm^{-1} represent the stretching vibrations of O-H groups from the surface of Fe_3O_4, which are bound to oleic acid, and hydrogen bonding interactions between MAA and IBP. The absorption band at 2922 cm^{-1} in all spectra originates from the stretching vibration of C-H groups in oleic acid and constituents of MMIPs and MNIPs. Peaks at 1708 and 1701 cm^{-1} indicate the vibrations of C=O bonds, and the absorption band at 1107 cm^{-1} in spectra (b) and (c) shows the vibrations of C-O bonds from methacrylic acid and IBP.

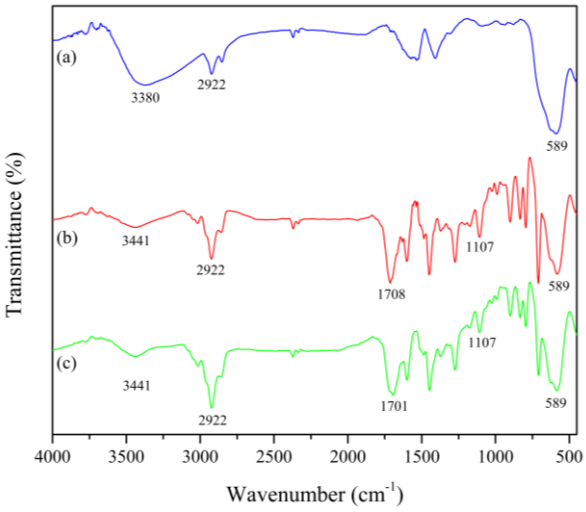

Figure 2. FTIR spectra of (a) Fe_3O_4 nanoparticles, (b) MNIPs, and (c) MMIPs

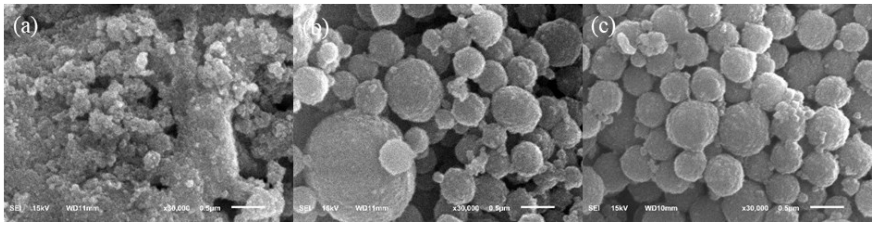

Figure 3. SEM images of (a) Fe_3O_4 nanoparticles, (b) MNIPs, and (c) MMIPs

3.3. Scanning Electron Microscope (SEM) Characterization

The morphology of Fe_3O_4 nanoparticles, MNIPs, and MMIPs was characterized using SEM. The SEM images are shown in Figure 3. The characterization results indicate that MNIPs and MMIPs have a spherical and homogeneous shape with relatively uniform size and specific cavities. This is due to the synthesis method, where the polymer is modified with Fe_3O_4 nanoparticles acting as the core of MMIPs to produce a regular and uniform shape. The use of Fe_3O_4 nanoparticles in the synthesis of MMIPs, modified in this way, results in nanosized MMIPs, enlarging the surface area of the adsorbent and yielding a high adsorption capacity. In contrast, the MMIPs synthesized using the precipitation polymerization method result in an irregular shape and require grinding [16].

3.4. Adsorption Isotherms

The study of adsorption isotherms was conducted to describe the interaction behavior between the adsorbate and adsorbent. The binding and adsorption properties of MMIPs for IBP are investigated by fitting the Langmuir and Freundlich adsorption isotherm models, as shown in Figure 4. The Langmuir isotherm model is described by Equation (3), which involves monolayer and homogeneous adsorption. This model assumes a uniform adsorbent surface and constant adsorption energy.

Additionally, the Langmuir model assumes that each active site on the adsorbent can only be occupied by one molecule, and there is no interaction between adsorbed molecules. The Freundlich model, described by Equation (4), is an empirical equation that can be applied to adsorption on heterogeneous surfaces and multilayer adsorption [19]. This model introduces a heterogeneity factor, 1/n, which characterizes surface heterogeneity [20]. The nonlinear form of the Langmuir and Freundlich isotherm models [19] is given by Equations (3) and (4).

$$q_e = \frac{K_L q_{max} C_e}{1+K_L C_e} \quad (3)$$

$$q_e = K_F C_e^{1/n} \quad (4)$$

In the Equations (3) and (4), q_e (mg/g) represents the amount of IBP adsorbed at equilibrium, C_e (mg/L) is the equilibrium concentration of IBP, K_L is the Langmuir binding constant related to adsorption energy, q_{max} (mg/g) is the maximum adsorption capacity of IBP, K_F is the Freundlich constant related to adsorption capacity, and 1/n is an indicator of exchange intensity or surface heterogeneity, with a value of 1/n less than 1.0 indicating favorable removal conditions. All constants are determined by fitting the equations [19].

Table 1. Langmuir and Freundlich isotherm model parameters

Langmuir			Freundlich		
q_{max} (mg/g)	K_L (L/mg)	R^2	K_f (L/mg)	n	R^2
227.24	0.0013	0.9862	0.4131	1.1239	0.9747

The IBP adsorption isotherm was determined using MMIPs at various concentrations, as shown in Figure 4, indicating that the adsorption capacity increases with the increase in IBP concentration. The parameters from both isotherm models calculated based on Equations (3) and (4) are presented in Table 1. Based on the results shown in Figure 4, the Langmuir isotherm model provides better results compared to the Freundlich isotherm model, as seen from the correlation coefficient (R^2) values, which are closer to 1 for the Langmuir isotherm model. Thus, it can be said that there is a homogeneous distribution of binding sites on the adsorbent surface, adsorption occurs in a monolayer, adsorbed molecules do not interact, and adsorption is reversible.

From the Langmuir adsorption isotherm calculations, the maximum adsorption capacity of IBP on MMIPs is 227.24 mg/g. This result is also supported by a study conducted by Sabín-López *et al.* [21], where molecularly imprinted polymers were synthesized to adsorb various contaminants, including IBP, which also followed the Langmuir adsorption isotherm model with an adsorption capacity of 26.58 mg/g.

3.5. Adsorption Kinetics

The study of adsorption kinetics was conducted to determine the adsorption rate and the equilibrium constant of the adsorption process. In this research, modeling of pseudo-first-order and pseudo-second-order kinetics was performed to investigate the mechanism of IBP adsorption onto MMIPs. The pseudo-first-order and pseudo-second-order kinetic models are represented by Equations (5) and (6), respectively [20].

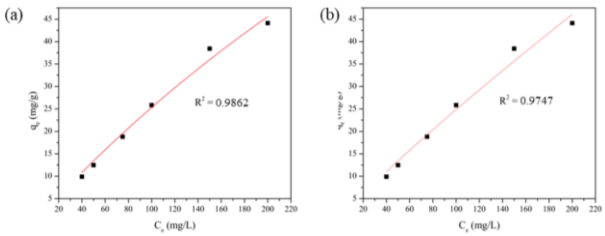

Figure 4. Non-linear fitting curve of IBP adsorption using MMIPs to (a) Langmuir isotherm model and (b) Freundlich isotherm model

Table 2. Parameters of pseudo-first-order and pseudo-second-order adsorption kinetic models

$q_{experiment}$ (mg/g)	Pseudo-first-order			Pseudo-second-order		
	K_1 (min^{-1})	$q_{theoretical}$ (mg/g)	R^2	K_2 (g/mg min)	$q_{theoretical}$ (mg/g)	R^2
15.6760	0.0306	13.9418	0.9260	0.0025	15.9744	0.9903

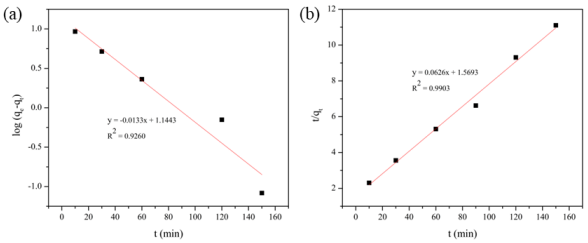

Figure 5. The linear fitting curve of IBP adsorption using MMIPs to (a) pseudo-first-order kinetic model and (b) pseudo-second-order-kinetic model

$$\log(q_e - q_t) = \log q_e - \frac{k_1 t}{2.303} \quad (5)$$

$$\frac{t}{q_t} = \frac{1}{k_2 q_e^2} + \frac{t}{q_e} \quad (6)$$

In Equations (5) and (6), q_t represents the amount of IBP adsorbed (mg/g) at t time (min), and k_1 (min^{-1}) and k_2 (g/mg/min) are the pseudo-first-order and pseudo-second-order rate constants, respectively. Both models can be interpreted with linear plots of log (q_e-q_t) vs. t and (t/q_t) vs. t, as shown in Figure 5. The rate constants k_1 and k_2 can be obtained from the experimental data plots [20].

All the fitting parameters are presented in Table 2. Based on Table 2, the pseudo-second-order kinetic model has an R^2 value of 0.9903, indicating a better fit than the pseudo-first-order kinetic model with an R^2 value of 0.9260. This suggests that the adsorption process follows the pseudo-second-order kinetic model, which describes the adsorption of IBP onto MMIPs, assuming the chemisorption events of the adsorbate on the adsorbent. The adsorption rate is controlled by a chemical adsorption mechanism involving electron exchange between the adsorbent and adsorbate [22]. This result is also supported by a study conducted by Sabín-López *et al.* [21], where molecularly imprinted polymers were synthesized for IBP adsorption and followed the pseudo-second-order kinetic adsorption model.

3.6. Selectivity Studies

The selectivity studies were conducted to determine the specific recognition ability of the MMIPs adsorbent for IBP. The test was performed with interfering compounds with characteristics similar to the analyte, in this case, a chemical derivative of propionic acid, namely NPX. Figure 6 illustrates the selectivity efficiency of MMIPs for IBP in the presence of the interfering compound NPX.

As depicted in Figure 6, MMIPs show a significantly higher adsorption capacity for IBP, even in the presence of the interfering compound in single and binary solutions with varying concentrations. This is because the complementary sites in the form of imprinted IBP cavities on MMIPs provide good selectivity to recognize and bind the target molecule. NPX is a propionic acid derivative larger than IBP, containing two benzene rings and an ether group. These characteristics can reduce the number of interactions with the designed IBP-imprinted cavities on MMIPs, causing NPX to have less effective interactions and thus lowering the adsorption efficiency for NPX molecules [23].

3.7. Regeneration Studies

The MMIPs adsorbent has an advantage in the separation process from the solution after the adsorption process because it only requires the assistance of an external magnetic field. This is crucial for the utilization of the adsorbent for repeated use. To assess the regeneration ability and stability of the prepared polymer, four cycles of adsorption-desorption experiments were conducted using a desorption solvent consisting of a MeOH:ACN solution mixture (1:1, v/v).

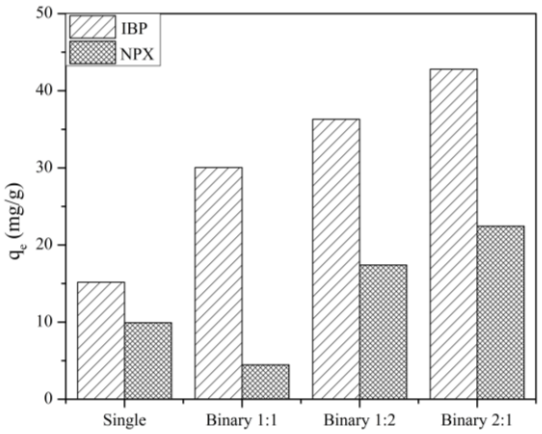

Figure 6. Selectivity of MMIPs toward IBP

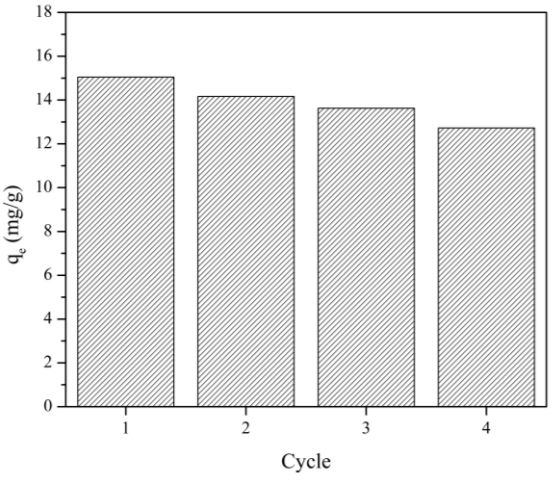

Figure 7. Regeneration of MMIPs

Figure 7 shows that the MMIPs adsorbent has good regeneration ability, with only a 15.5% decrease in adsorption capacity after four polymer regeneration cycles. The decrease in adsorption capacity in MMIPs can be attributed to potential changes in the number of active sites on the polymer surface due to washing, as indicated by black uncoated magnetite particles during washing. Additionally, some polymer cavities may have been filled with target molecules and are challenging to desorb, thus affecting subsequent adsorption processes. However, the results of this study indicate that MMIPs have good reusability and can be easily regenerated for further use [23].

4. Conclusion

Magnetic molecularly imprinted polymers (MMIPs) were synthesized using the bulk polymerization method and characterized through XRD, FTIR, and SEM. Isotherm adsorption studies revealed that IBP adsorption onto MMIPs follows a monolayer adsorption mechanism on a homogeneous surface, as described by the Langmuir model. Kinetic studies indicated that the adsorption process follows a pseudo-second-order kinetic equation. In selective recognition experiments, MMIPs exhibited better recognition and specific selectivity towards IBP, even in the presence of interfering compounds in single and mixed solutions. Furthermore, regeneration studies demonstrated that MMIPs can be reused multiple times for IBP removal without significantly decreasing adsorption capacity.

Acknowledgment

The author would like to express gratitude towards Institut Teknologi Bandung, Faculty of Mathematics and Natural Sciences, Department of Chemistry, for facilitating this work.

References

[1] Lawrence Mzukisi Madikizela, Luke Chimuka, Synthesis, adsorption and selectivity studies of a polymer imprinted with naproxen, ibuprofen and diclofenac, *Journal of Environmental Chemical Engineering*, 4, 4, (2016), 4029-4037 https://doi.org/10.1016/j.jece.2016.09.012

[2] Nurlin Abu Samah, María-Jesús Sánchez-Martín, Rosa Mª Sebastián, Manuel Valiente, Montserrat López-Mesas, Molecularly imprinted polymer for the removal of diclofenac from water: Synthesis and characterization, *Science of The Total Environment*, 631-632, (2018), 1534-1543 https://doi.org/10.1016/j.scitotenv.2018.03.087

[3] Omar Israel González Peña, Miguel Ángel López Zavala, Héctor Cabral Ruelas, Pharmaceuticals Market, Consumption Trends and Disease Incidence are Not Driving the Pharmaceutical Research on Water and Wastewater, *International Journal of Environmental Research and Public Health*, 18, 5, (2021), 2532

[4] Marit Huizer, Thomas L. ter Laak, Pim de Voogt, Annemarie P. van Wezel, Wastewater-based epidemiology for illicit drugs: A critical review on global data, *Water Research*, 207, (2021), 117789 https://doi.org/10.1016/j.watres.2021.117789

[5] A. I. Moral-Rodriguez, R. Leyva-Ramos, F. Carrasco-Marín, M. I. Bautista-Toledo, A. F. Pérez-Cadenas, Adsorption of Diclofenac from Aqueous Solution onto Carbon Xerogels: Effect of Synthesis Conditions and Presence of Bacteria, *Water, Air, & Soil Pollution*, 231, 1, (2020), 17 https://doi.org/10.1007/s11270-019-4385-5

[6] Osama Abrahiem Al Falahi, Siti Rozaimah Sheikh Abdullah, Hassimi Abu Hasan, Ahmad Razi Othman, Hind Mufeed Ewadh, Israa Abdulwahab Al-Baldawi, Setyo Budi Kurniawan, Muhammad Fauzul Imron, Nur 'Izzati Ismail, Simultaneous removal of ibuprofen, organic material, and nutrients from domestic wastewater through a pilot-scale vertical sub-surface flow constructed wetland with aeration system, *Journal of Water Process Engineering*, 43, (2021), 102214 https://doi.org/10.1016/j.jwpe.2021.102214

[7] Oya Irmak Sahin, Berrin Saygi-Yalcin, Didem Saloglu, Adsorption of ibuprofen from wastewater using activated carbon and graphene oxide embedded chitosan–PVA: equilibrium, kinetics, and thermodynamics and optimization with central composite design, *Desalination and Water Treatment*, 179, (2020), 396-417 https://doi.org/10.5004/dwt.2020.25027

[8] Joanna Lach, Anna Szymonik, Adsorption of diclofenac sodium from aqueous solutions on commercial activated carbons, *Desalination And Water Treatment*, 186, (2020), 418-429 https://doi.org/10.5004/dwt.2020.25567

[9] Stephen N. Oba, Joshua O. Ighalo, Chukwunonso O. Aniagor, Chinenye Adaobi Igwegbe, Removal of ibuprofen from aqueous media by adsorption: A comprehensive review, *Science of The Total Environment*, 780, (2021), 146608 https://doi.org/10.1016/j.scitotenv.2021.146608

[10] Chao-meng Dai, Sven-Uwe Geissen, Ya-lei Zhang, Yong-jun Zhang, Xue-fei Zhou, Selective removal of diclofenac from contaminated water using molecularly imprinted polymer microspheres, *Environmental Pollution*, 159, 6, (2011), 1660-1666 https://doi.org/10.1016/j.envpol.2011.02.041

[11] St. Fauziah, N. H. Soekamto, P. Budi, P. Taba, Adsorption Capacity and Selectivity of Molecularly Imprinted Polymers towards β -Sitosterol, *Asian Journal of Chemistry*, 31, 11, (2019), 2527-2531 https://doi.org/10.14233/ajchem.2019.22141

[12] Nor Aniisah Husin, Musthahimah Muhamad, Noorfatimah Yahaya, Mazidatulakmam Miskam, Nik Nur Syazni Nik Mohamed Kamal, Saliza Asman, Muggundha Raoov, Nur Nadhirah Mohamad Zain, Application of a new choline-imidazole based deep eutectic solvents in hybrid magnetic molecularly imprinted polymer for efficient and selective removal of naproxen from aqueous samples, *Materials Chemistry and Physics*, 261, (2021), 124228 https://doi.org/10.1016/j.matchemphys.2021.124228

[13] Qiang Xia, Yanbin Yun, Qiang Li, Zejun Huang, Zhixia Liang, Preparation and characterization of monodisperse molecularly imprinted polymer microspheres by precipitation polymerization for kaempferol, *Designed Monomers and Polymers*, 20, 1, (2017), 201-209 https://doi.org/10.1080/15685551.2016.1239174

[14] Rosario Josefina Uzuriaga-Sánchez, Ademar Wong, Sabir Khan, Maria I. Pividori, Gino Picasso, Maria D. P. T Sotomayor, Synthesis of a new magnetic-MIP for the selective detection of 1-chloro-2, 4-dinitrobenzene, a highly allergenic compound, *Materials Science and Engineering: C*, 74, (2017), 365-373 https://doi.org/10.1016/j.msec.2016.12.019

[15] Saeedeh Ansari, Majid Karimi, Recent configurations and progressive uses of magnetic molecularly imprinted polymers for drug analysis, *Talanta*, 167, (2017), 470-485 https://doi.org/10.1016/j.talanta.2017.02.049

[16] Rizqi Utami Asyifa, Ali Zulfikar Muhammad, Deana Wahyuningrum, The synthesis of magnetic molecularly imprinted polymer against di-(2-ethylhexyl)phthalate, *IOP Conference Series: Materials Science and Engineering*, 1143, 1, (2021), 012003 https://doi.org/10.1088/1757-899X/1143/1/012003

[17] Djabal Nur Basir, Muhammad Ali Zulfikar, Muhammad Bachri Amran, The synthesis of imprinted polymer sorbent for the removal of mercury ions, *Songklanakarin Journal of Science & Technology*, 42, 5, (2020), 1135-1141

[18] K. Petcharoen, A. Sirivat, Synthesis and characterization of magnetite nanoparticles via the chemical co-precipitation method, *Materials Science and Engineering: B*, 177, 5, (2012), 421-427 https://doi.org/10.1016/j.mseb.2012.01.003

[19] Jian Zhang, Changpo Ma, Hui Li, Ximo Wang, Feng Ning, Minxia Kang, Zumin Qiu, Polyethyleneimine Modified Magnetic Microcrystalline Cellulose for Effective Removal of Congo Red: Adsorption Properties and Mechanisms, *Fibers and Polymers*, 22, (2021), 1580-1593 https://doi.org/10.1007/s12221-021-0543-7

[20] M. A. Zulfikar, D. Wahyuningrum, R. R. Mukti, H. Setiyanto, Molecularly imprinted polymers (MIPs): a functional material for removal of humic acid from peat water, *Desalination and Water Treatment*, 57, 32, (2016), 15164-15175 https://doi.org/10.1080/19443994.2015.1069218

[21] Alejandra Sabín-López, María Paredes Ramos, Roberto Herrero, Jose Manuel López Vilariño, Synthesis of magnetic green nanoparticle – Molecular imprinted polymers with emerging contaminants templates, *Journal of Environmental Chemical Engineering*, 8, 4, (2020), 103889 https://doi.org/10.1016/j.jece.2020.103889

[22] Yanli Mao, Jiuyun Cui, Juan Zhao, Yilin Wu, Chen Wang, Jian Lu, Xinyu Lin, Yongsheng Yan, Selective separation of bifenthrin by pH-sensitive/magnetic molecularly imprinted polymers prepared by pickering emulsion polymerization, *Fibers and Polymers*, 17, 10, (2016), 1531-1539 https://doi.org/10.1007/s12221-016-6570-0

[23] Muhammad Ali Zulfikar, Asyifa Rizqi Utami, Nurrahmi Handayani, Deana Wahyuningrum, Henry Setiyanto, Muhammad Yudhistira Azis, Removal of phthalate ester compound from PVC plastic samples using magnetic molecularly imprinted polymer on the surface of superparamagnetic Fe_3O_4 (Fe_3O_4@MIPs), *Environmental Nanotechnology, Monitoring & Management*, 17, (2022), 100646 https://doi.org/10.1016/j.enmm.2022.100646